

Supporting information

Table S1. Tensor parameters and shift of metal ion from starting position for the 10 subsets (from a total of 100) resulting in the largest number of peak pairings, using 2D and 3D data of $^{15}\text{N}/^{13}\text{C}$ - $\epsilon 186/\theta$ complexed with Dy^{3+} , Er^{3+} and Tb^{3+} , respectively, and their diamagnetic reference spectra.

2D $\epsilon 186/\theta/\text{Dy}^{3+}$							3D $\epsilon 186/\theta/\text{Dy}^{3+}$						
#peaks	$\Delta\chi_{\text{ax}}$	$\Delta\chi_{\text{rh}}$	α/deg	β/deg	γ/deg	$d/\text{\AA}$	#peaks	$\Delta\chi_{\text{ax}}$	$\Delta\chi_{\text{rh}}$	α/deg	β/deg	γ/deg	$d/\text{\AA}$
37	40.0	5.8	25	78	14	0.9	46	39.4	4.0	27	79	23	0.7
34	37.8	6.1	27	76	27	1.1	45	36.8	3.5	26	78	31	1.0
32	29.2	1.3	23	81	69	2.0	45	39.3	4.5	27	79	21	0.7
31	39.5	6.0	26	78	18	0.8	43	36.8	3.5	26	78	29	1.0
30	33.0	5.2	25	77	17	1.6	43	38.6	4.5	28	78	28	0.7
29	34.3	6.5	27	85	135	2.1	42	34.0	2.5	26	79	36	1.1
29	32.7	0.9	23	86	163	2.4	40	38.2	4.1	27	79	29	0.7
28	34.1	1.4	22	81	156	1.7	39	40.6	3.2	29	79	18	0.7
28	24.0	0.7	23	87	144	3.3	39	39.9	0.3	27	79	47	0.5
28	43.3	6.8	28	79	16	1.0	38	37.5	5.2	25	79	8	1.1

2D $\epsilon 186/\theta/\text{Er}^{3+}$							3D $\epsilon 186/\theta/\text{Er}^{3+}$						
#peaks	$\Delta\chi_{\text{ax}}$	$\Delta\chi_{\text{rh}}$	α/deg	β/deg	γ/deg	$d/\text{\AA}$	#peaks	$\Delta\chi_{\text{ax}}$	$\Delta\chi_{\text{rh}}$	α/deg	β/deg	γ/deg	$d/\text{\AA}$
77	-11.1	-4.0	24	90	41	0.4	78	-10.5	-4.3	24	90	41	0.6
77	-10.8	-3.4	25	91	44	0.2	78	-10.5	-4.4	23	91	40	0.8
77	-10.4	-3.9	22	91	46	0.8	78	-10.5	-4.4	23	91	40	0.8
77	-10.4	-3.6	23	90	47	0.8	78	-10.5	-4.3	23	91	41	0.7
76	-11.4	-4.1	24	90	41	0.6	78	-10.5	-4.3	23	91	41	0.7
76	-11.2	-4.0	23	91	42	0.6	78	-10.5	-4.3	23	91	41	0.7
76	-11.1	-4.0	24	90	41	0.5	78	-10.5	-4.5	23	90	42	0.8
76	-11.1	-3.9	23	91	42	0.6	78	-10.5	-4.5	23	90	42	0.8
76	-11.0	-3.8	23	91	43	0.5	78	-10.5	-4.5	23	90	42	0.8
76	-10.9	-3.6	23	92	43	0.5	78	-10.5	-4.4	23	90	42	0.8

2D $\epsilon 186/\theta/\text{Tb}^{3+}$							3D $\epsilon 186/\theta/\text{Tb}^{3+}$						
#peaks	$\Delta\chi_{\text{ax}}$	$\Delta\chi_{\text{rh}}$	α/deg	β/deg	γ/deg	$d/\text{\AA}$	#peaks	$\Delta\chi_{\text{ax}}$	$\Delta\chi_{\text{rh}}$	α/deg	β/deg	γ/deg	$d/\text{\AA}$
56	27.7	3.7	19	84	3	0.6	63	27.8	5.9	20	84	0	0.7
55	27.9	4.0	19	84	4	0.7	63	27.6	5.8	20	84	0	0.7
54	28.6	4.8	20	84	-3	0.5	63	27.6	5.8	20	84	0	0.7
53	28.0	5.1	18	85	2	1.3	63	27.3	5.7	20	84	0	0.8
52	29.5	5.2	20	84	6	0.7	63	27.3	5.7	20	84	-1	0.7
52	27.5	4.7	17	85	2	1.2	63	27.3	5.7	20	84	0	0.7
51	29.7	6.4	20	85	-1	0.6	63	27.3	5.7	20	84	0	0.7
50	27.1	3.0	22	84	-10	0.2	63	27.3	5.7	20	84	0	0.7
49	28.1	4.7	20	85	-13	1.0	62	27.9	5.6	20	84	-3	0.7
49	27.9	4.7	20	85	-11	0.8	62	27.6	5.8	20	84	1	0.7

Table S2. Tensor parameters determined by Echidna for randomly varied structures, using 2D data of $^{15}\text{N}/^{13}\text{C}$ - ϵ 186/ θ complexed with Dy^{3+} , Er^{3+} and Tb^{3+} , respectively, and the diamagnetic reference. Structural variation was obtained by random displacement of the N and H atomic coordinates following a Gaussian distribution with $\sigma = 0.5, 1.0, 1.5$ and 2.0 \AA along each coordinate. Tensors and paramagnetic resonance assignments were determined using Echidna for 10 different randomized structures.

2D ϵ 186/ θ / Dy^{3+} $\sigma = 0.5 \text{ \AA}$						2D ϵ 186/ θ / Dy^{3+} $\sigma = 1.0 \text{ \AA}$					
#peaks	$\Delta\chi_{\text{ax}}$	$\Delta\chi_{\text{rh}}$	α/deg	β/deg	γ/deg	#peaks	$\Delta\chi_{\text{ax}}$	$\Delta\chi_{\text{rh}}$	α/deg	β/deg	γ/deg
30	34.6	4.2	23	79	26	22	27.2	2.9	25	81	44
30	34.5	4.1	28	80	154	20	20.4	1.3	28	76	86
28	40.9	2.0	27	77	153	20	36.8	15.7	29	77	38
28	33.3	3.6	27	83	35	19	42.0	5.3	30	78	150
28	36.1	3.7	28	79	126	18	25.7	1.1	23	83	4
26	39.3	5.4	33	84	41	18	27.1	12.9	22	91	134
25	24.0	2.0	23	89	129	17	20.7	5.0	20	93	73
25	30.4	1.1	25	81	16	16	41.5	18.9	26	80	18
25	39.1	3.8	29	78	176	9	51.5	29.7	18	81	146
24	36.9	8.3	27	78	30	5	2.1	1.1	0	1	2
2D ϵ 186/ θ / Er^{3+} $\sigma = 0.5 \text{ \AA}$						2D ϵ 186/ θ / Er^{3+} $\sigma = 1.0 \text{ \AA}$					
#peaks	$\Delta\chi_{\text{ax}}$	$\Delta\chi_{\text{rh}}$	α/deg	β/deg	γ/deg	#peaks	$\Delta\chi_{\text{ax}}$	$\Delta\chi_{\text{rh}}$	α/deg	β/deg	γ/deg
76	-10.2	-4.0	24	89	43	65	-10.9	-4.4	30	90	37
74	-11.5	-5.5	24	89	40	61	-10.9	-2.9	23	91	41
73	-10.9	-4.3	24	90	44	60	-12.3	-7.7	20	84	46
72	-10.7	-3.9	22	90	38	60	-11.2	-4.8	21	90	37
71	-10.0	-3.9	21	91	44	59	-10.9	-1.8	25	89	40
71	-10.5	-3.6	25	88	44	59	-9.1	-4.2	22	91	44
71	-10.0	-3.4	25	90	40	59	-10.8	-4.1	22	89	41
70	-10.6	-4.2	22	91	31	57	-10.0	-1.3	24	94	52
68	-10.3	-3.9	22	92	34	57	-11.2	-3.9	25	90	33
64	-10.3	-5.7	22	87	41	57	-9.4	-4.5	25	86	44
2D ϵ 186/ θ / Tb^{3+} $\sigma = 0.5 \text{ \AA}$						2D ϵ 186/ θ / Tb^{3+} $\sigma = 1.0 \text{ \AA}$					
#peaks	$\Delta\chi_{\text{ax}}$	$\Delta\chi_{\text{rh}}$	α/deg	β/deg	γ/deg	#peaks	$\Delta\chi_{\text{ax}}$	$\Delta\chi_{\text{rh}}$	α/deg	β/deg	γ/deg
49	24.3	4.7	21	84	9	37	27.0	4.5	22	81	4
48	28.8	6.5	21	84	11	35	29.3	6.0	23	83	178
47	22.6	4.1	18	86	11	33	29.2	7.7	21	84	170
47	26.6	6.8	20	83	13	33	24.8	6.7	20	82	5
45	24.9	3.6	18	86	14	32	18.2	1.0	25	86	38
45	24.9	4.2	20	84	12	32	26.6	4.8	23	85	177
44	25.3	5.1	19	84	12	31	20.7	3.0	21	87	14
43	22.8	4.6	24	84	10	31	19.4	1.1	13	83	27
42	23.5	4.2	21	84	27	29	22.2	3.4	21	79	166
40	25.8	5.6	20	86	12	27	18.2	4.7	27	84	127

2D $\epsilon 186/\theta/\text{Dy}^{3+}$ $\sigma = 1.5 \text{ \AA}$						2D $\epsilon 186/\theta/\text{Dy}^{3+}$ $\sigma = 2.0 \text{ \AA}$					
#peaks	$\Delta\chi_{ax}$	$\Delta\chi_{rh}$	α/deg	β/deg	γ/deg	#peaks	$\Delta\chi_{ax}$	$\Delta\chi_{rh}$	α/deg	β/deg	γ/deg
19	18.3	8.5	29	85	137	14	19.4	2.4	7	92	46
16	18.5	6.4	24	111	52	14	18.0	4.6	35	84	62
16	39.1	17.8	24	84	156	10	15.2	8.9	42	74	33
15	21.2	10.9	23	84	122	9	2.3	30.3	111	132	177
14	27.6	12.3	30	81	125	7	-2.3	4.3	0	0	0
8	34.2	26.2	50	128	164	5	0.4	37.9	-17	167	30
8	56.5	55.4	18	93	116	5	29.3	20.8	27	90	43
7	42.8	16.5	15	89	85	5	6.3	1.7	-1	2	101
6	73.3	49.9	161	98	4	5	16.7	7.0	50	153	102
2	90.4	42.8	28	98	164	3	0.5	0.1	0	0	179
2D $\epsilon 186/\theta/\text{Er}^{3+}$ $\sigma = 1.5 \text{ \AA}$						2D $\epsilon 186/\theta/\text{Er}^{3+}$ $\sigma = 2.0 \text{ \AA}$					
#peaks	$\Delta\chi_{ax}$	$\Delta\chi_{rh}$	α/deg	β/deg	γ/deg	#peaks	$\Delta\chi_{ax}$	$\Delta\chi_{rh}$	α/deg	β/deg	γ/deg
56	-12.5	-4.2	24	90	40	47	-9.7	-3.2	20	95	36
54	-10.2	-4.4	27	90	43	45	-8.0	-2.3	11	90	65
52	-11.2	-7.6	25	84	41	45	-8.5	-5.7	22	94	42
52	-8.4	-5.1	25	99	50	44	-9.7	-4.0	20	84	35
51	-10.1	-4.8	21	90	46	44	-9.7	-3.8	23	100	30
50	-9.8	-4.9	23	88	43	43	-7.1	-4.9	24	91	46
47	-10.5	-2.8	24	88	26	43	-10.5	-4.4	24	88	40
47	-9.8	-6.6	16	96	48	41	-10.4	-2.8	20	96	46
45	-10.0	-5.6	22	88	29	40	-10.5	-2.9	24	84	35
44	-10.9	-2.3	23	86	19	39	-4.2	-4.0	17	91	48
2D $\epsilon 186/\theta/\text{Tb}^{3+}$ $\sigma = 1.5 \text{ \AA}$						2D $\epsilon 186/\theta/\text{Tb}^{3+}$ $\sigma = 2.0 \text{ \AA}$					
#peaks	$\Delta\chi_{ax}$	$\Delta\chi_{rh}$	α/deg	β/deg	γ/deg	#peaks	$\Delta\chi_{ax}$	$\Delta\chi_{rh}$	α/deg	β/deg	γ/deg
31	21.8	4.2	24	86	14	28	21.0	7.1	27	79	146
30	17.1	2.8	21	90	26	26	17.8	5.8	23	87	19
30	11.6	2.6	15	79	150	25	14.6	1.7	11	83	108
29	29.2	8.2	24	78	167	24	20.3	4.3	26	79	139
28	17.3	4.7	30	84	32	22	16.8	2.3	23	74	22
25	16.4	0.2	18	75	54	21	10.9	1.9	19	90	146
25	20.1	0.8	17	91	159	21	16.0	6.9	28	64	60
22	22.5	5.0	26	86	133	20	13.1	8.7	-1	163	33
21	22.4	6.7	25	80	158	9	43.1	143.7	81	134	138
9	42.8	14.8	35	56	191	6	57.5	23.7	-3	66	97

Figure S1. Results of Table S2 visualized in Sanson-Flamsteed projections, with the principal axes of the magnetic susceptibility tensors shown in brown (x-axis), purple (y-axis) and blue (z-axis). The crystal coordinates (PDB code 1J53) were used as the reference coordinate system. No results are shown for cases where the number of initial peak pairings was below 10, since a minimum of 10 initial assignments was the requirement for random subset sampling.

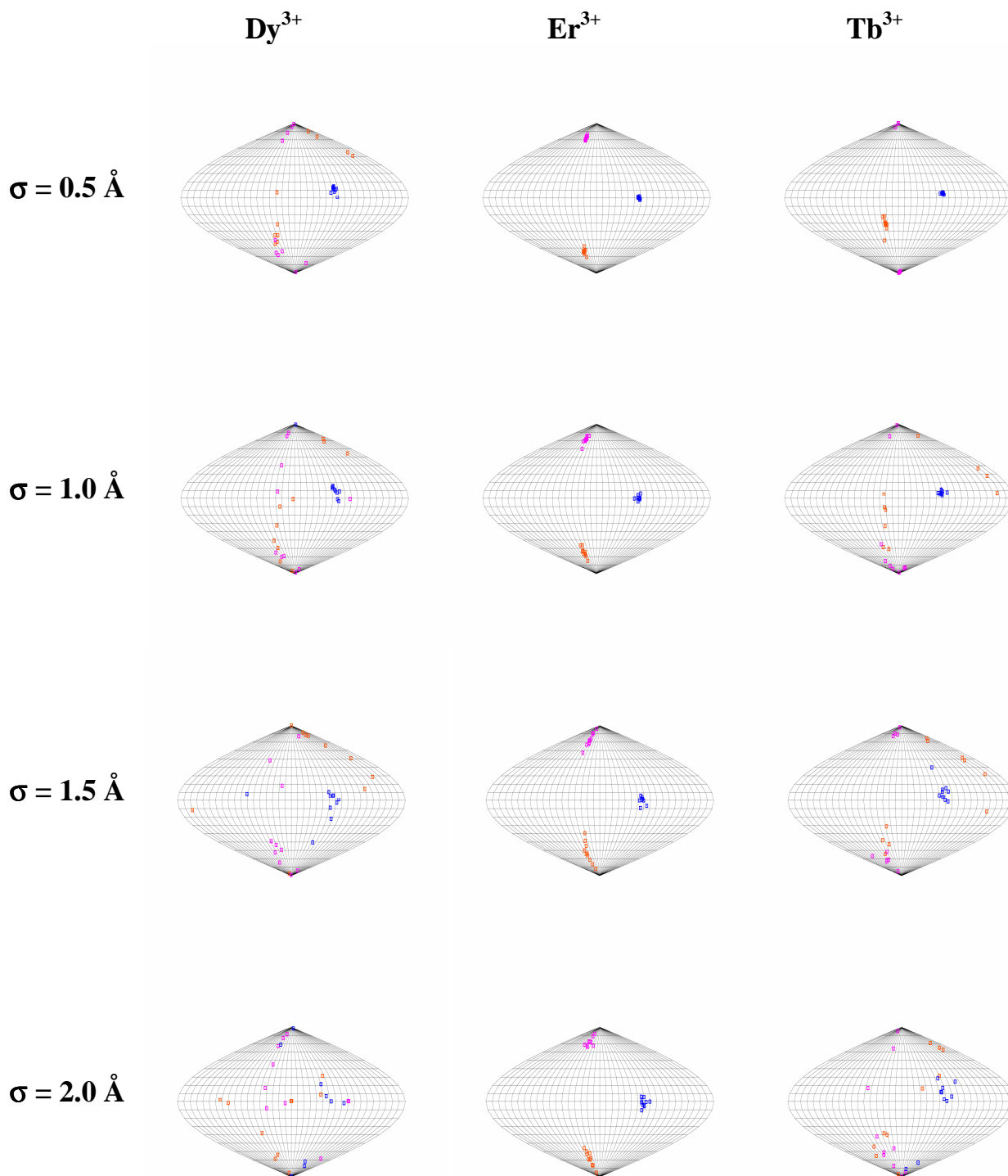


Table S3. Chemical shifts of $^{15}\text{N}/^{13}\text{C}$ -labeled $\epsilon 186$ complexed to unlabeled θ and different lanthanide ions at pH 7.2 and 25 °C.^a

residue	diamagnetic (La)			paramagnetic (Dy)			paramagnetic (Er)			paramagnetic (Tb)		
	C'	N	HN	C'	N	HN	C'	N	HN	C'	N	HN
1 MET												
2 SER												
3 THR	174.1			174.1			174.1			174.2		
4 ALA	177.3	127.1	8.43	177.3	127.1	8.43	177.4	127.1	8.46	177.4	127.2	8.51
5 ILE	176.7	121.3	8.33	176.6	121.2	8.30	176.8	121.3	8.37	176.8	121.3	8.41
6 THR	173.4	119.8	8.59	173.5	119.9	8.61	173.5	119.9	8.65	173.7	120.0	8.73
7 ARG	174.2	125.6	8.26	174.0	125.5	8.11	174.5	125.8	8.40	174.3	125.7	8.35
8 GLN	174.5	124.9	9.36		124.9	9.41	174.8	125.1	9.54	174.8	125.1	9.65
9 ILE	174.1	122.5	9.14				123.0	9.60			122.5	9.21
10 VAL	175.7	129.7	9.02									
11 LEU		126.6	8.49									
12 ASP	173.8											
13 THR	174.7	114.5	8.01									
14 GLU	177.6	118.5	8.79									
15 THR	174.1	111.2	8.94									
16 THR	172.0	107.5	8.97									
17 GLY	170.6	104.9	7.64									
18 MET	173.6	113.4	7.90				173.4					
19 ASN	175.8	119.0	9.09				175.8	118.7	8.86			
20 GLN	175.3	121.6	9.02				175.3	121.6	9.01	174.8		
21 ILE	175.4	117.1	7.57	175.4			175.5	117.0	7.59	175.1	116.6	7.36
22 GLY	173.4	112.1	8.29	173.4	112.1	8.21	173.4	112.1	8.34	173.0	111.7	7.93
23 ALA	181.3	124.5	8.36	181.7	124.8	8.53	181.3	124.5	8.34	181.0	124.3	8.15
24 HIS		121.5	8.33		121.6	8.15		121.6	8.39		121.1	7.66
25 TYR	174.7			176.6						175.3		
26 GLU	177.5	120.6	5.60	179.1	122.0	6.69	177.2			178.2	121.0	5.77
27 GLY	173.2	111.8	8.15	175.9	113.5	9.80	172.6	111.5	7.82	174.6	112.6	8.88
28 HIS	173.6	120.9	8.48		123.7	11.17		120.3	7.95		122.4	9.73
29 LYS	177.2	113.4	8.52									
30 ILE	175.7	121.6	9.65									
31 ILE	174.7	117.1	8.89									
32 GLU	174.8	122.6	7.47									
33 ILE	174.0	124.6	8.60									
34 GLY	170.9	115.5	9.28									
35 ALA	175.6	125.3	9.54									
36 VAL	174.4	113.8	8.83				175.5			174.0		
37 GLU	175.2	121.7	6.48	175.5			175.6	122.6	7.31	175.5	121.3	5.79
38 VAL	175.2	130.2	9.57	175.6	130.5	9.64	175.4	130.4	9.88	175.6	130.5	9.84
39 VAL	177.0	125.5	8.94	177.6	125.8	9.40	177.0	125.6	9.02	177.5	125.8	9.32
40 ASN	174.3	128.6	9.46	174.9	129.1	9.81	174.3	128.6	9.48	174.8	129.0	9.81
41 ARG	173.1	106.3	8.96	174.2	107.1	9.70	173.1	106.1	8.87	173.9	106.9	9.59
42 ARG	175.1	117.3	7.68	176.2	118.2	8.48	175.1	117.2	7.63	175.8	117.9	8.27
43 LEU	178.7	125.6	8.78	179.2	126.8	9.99	178.9	125.6	8.69	178.9	126.3	9.49
44 THR	177.2	114.7	7.84	177.0	114.9	8.07	177.4	115.0	8.08	176.9	114.7	7.93
45 GLY	173.9	111.7	9.96	173.1	111.3	9.82	174.4	112.0	10.32	173.2	111.3	9.69
46 ASN	173.3	119.7	8.02	171.7	119.0	7.30	174.1	120.2	8.48	172.1	119.1	7.43
47 ASN	174.1	123.6	7.68		121.6	5.83		124.5	8.49		122.1	6.25
48 PHE	172.9	122.0	9.15									
49 HIS	172.8	127.0	7.54									
50 VAL	172.8	119.7	8.53									
51 TYR		119.2	8.04									
52 LEU	174.3						173.3					
53 LYS		120.8	8.31					120.0	7.67			
54 PRO												
55 ASP												
56 ARG	174.5			177.8			173.8			176.7		
57 LEU	178.5	120.0	8.73		123.3	11.62	177.4	119.2	8.02		122.1	10.60
58 VAL	176.0	125.5	10.75					124.3	9.57			
59 ASP		128.8	9.25									
60 PRO	178.7											

paramagnetic spectra was greatly reduced due to paramagnetic relaxation enhancement. Observable cross-peaks were from amide protons located beyond a certain cutoff distance r_{cutoff} from the metal ion. This distance was about 15.5 Å for Dy³⁺, and 15.0 Å for Tb³⁺ and Er³⁺. In all three cases, an initial set of 15 to 20 peaks could be identified that were shifted from well-resolved cross-peaks in the diamagnetic HNCO spectrum by similar ppm values in all three dimensions. The pseudocontact shifts (PCS) derived from these paramagnetic/diamagnetic peak pairs were used to fit the $\Delta\chi$ tensor parameters and predict PCS values for all ¹³C, ¹⁵N, and ¹H^N nuclei in ε186 using Mathematica (Wolfram Research) routines. This allowed the identification of new assignments. The procedure was repeated iteratively and resulted in the confident assignment of 77 out of 81 HNCO peaks for the Dy³⁺, 97 out of 104 HNCO peaks for the Er³⁺, and 77 out of 89 HNCO peaks for the Tb³⁺ sample, respectively.